High expression of cytochrome b_5 reductase isoform 3/cytochrome b_5 system in the cerebellum and pyramidal neurons of adult rat brain

A. K. Samhan-Arias [1]

C. López-Sánchez [2]

D. Marques-da-Silva [1]

R. Lagoa [1,2,3]

V. Garcia-Lopez [4]

V. García-Martínez [2]

C. Gutierrez-Merino [1,*]

Phone +34924289419
Email carlosgm@unex.es

[1] Department of Biochemistry and Molecular Biology, Faculty of Sciences, University of Extremadura, 06006 Badajoz, Spain

[2] Department of Human Anatomy and Embryology, Faculty of Medicine, University of Extremadura, 06006 Badajoz, Spain

[3] ESTG-Polytechnic Institute of Leiria, Leiria, Portugal

[4] Minimally Invasive Surgery Centre, Cáceres, Spain

Abstract

Cytochrome b_5 reductase (Cb_5R) and cytochrome b_5 (Cb_5) form an enzymatic redox system that plays many roles in mammalian cells. In the last 15 years, it has been proposed that this system is involved in the recycling of ascorbate, a vital antioxidant molecule in the brain and that its

deregulation can lead to the production of reactive oxygen species that play a major role in oxidative-induced neuronal death. In this work, we have performed a regional and cellular distribution study of the expression of this redox system in adult rat brain by anti-Cb_5R isoform 3 and anti-Cb_5 antibodies. We found high expression levels in cerebellar cortex, labeling heavily granule neurons and Purkinje cells, and in structures such as the fastigial, interposed and dentate cerebellar nuclei. A large part of Cb_5R isoform 3 in the cerebellum cortex was regionalized in close proximity to the lipid raft-like nanodomains, labeled with cholera toxin B, as we have shown by fluorescence resonance energy transfer imaging. In addition, vestibular, reticular and motor nuclei located at the brain stem level and pyramidal neurons of somatomotor areas of the brain cortex and of the hippocampus have been also found to display high expression levels of these proteins. All these results point out the enrichment of Cb_5R isoform 3/Cb_5 system in neuronal cells and structures of the cerebellum and brain stem whose functional impairment can account for neurological deficits reported in type II congenital methemoglobinemia, as well as in brain areas highly prone to undergo oxidative stress-induced neurodegeneration.

Keywords

Cytochrome b_5
Cytochrome b_5 reductase isoform 3
Rat brain
Cerebellum
Brain stem
Purkinje neurons
Cerebellar granule neurons
Cerebellar and vestibular nuclei
Hippocampus
Neocortex

A. K. Samhan-Arias and C. López-Sánchez equally contributed to this work and should be considered first authors.

Electronic supplementary material

The online version of this article (doi:10.1007/s00429-015-1036-5) contains supplementary material, which is available to authorized users.

Introduction

The redox enzyme system cytochrome b_5 reductase (Cb_5R)/cytochrome b_5 (Cb_5) plays a pleiotropic role in cell biology. Major cellular functions, which are dependent on this system, include biosynthesis of unsaturated fatty acids (Jeffcoat et al. 1977; Rioux et al. 2011), regulation of the biosynthesis of cholesterol (Kawata et al. 1985), modulation of cytochrome P450 isoforms involved in the biosynthesis of steroid hormones and xenobiotics detoxification (Hildebrandt and Estabrook 1971; Schenkman and Jansson 2003) and reduction/recycling of methemoglobin (Hultquist and Passon 1971; Leroux et al. 1975; Vieira et al. 1995). In addition, Cb_5R is a component of the plasma redox membrane chain (Villalba et al. 1997; May 1999; Samhan-Arias et al. 2008), and this system has been involved in the recycling of ascorbate free radical to ascorbate (May 1999; Samhan-Arias et al. 2008; Harrison and May 2009), one of the major antioxidant defenses in the brain. It has been described more than 40 naturally occurring mutations of the human Cb_5R, and more than 50 % of them produce recessive congenital methemoglobinemia of type II, an inherited disease where mild cyanosis is accompanied by severe neurological impairment and reduced life expectancy (Percy and Lappin 2008; Ewenczyk et al. 2008; Huang et al. 2012). In this rare disease, individuals show developmental delay, progressive microcephaly, generalized dystonia, movement disorders, failure to thrive, and cortical and subcortical atrophy (Leroux et al. 1975; Toelle et al. 2004; Percy and Lappin 2008; Ewenczyk et al. 2008; Huang et al. 2012), including cerebellar atrophy (Aalfs et al. 2000).

The apoptosis of cerebellar granule neurons in culture induced by low K^+ in the extracellular medium is a well-established model for the neuronal apoptosis observed during brain development (Contestabile 2002). Noteworthy, this model of neuronal apoptosis has been shown to be also valuable for molecular studies correlating apoptosis with events related to Alzheimer's disease (Canu and Calissano 2003). Deregulation of the redox chain of the plasma membrane can lead to a superoxide anion overshot, an early event in low K^+-induced apoptosis of cerebellar granule neurons which is critical for the advance of this apoptosis into the irreversible phase characterized by caspases activation (Valencia and Moran 2001; Martin-Romero et al. 2002; Samhan-Arias et al. 2004). We have shown that the stimulation of Cb_5R associated with the plasma membrane of cerebellar

granule neurons can account for most of the superoxide anion overshot produced before the entry into the irreversible phase of the apoptosis of these neurons (Samhan-Arias et al. 2009). Recently, we have shown that the production of superoxide anion coupled to the NADH oxidase activity of purified Cb_5R is inhibited by apocynin (Samhan-Arias and Gutierrez-Merino 2014a), a compound that has been extensively used as a 'selective' inhibitor of superoxide anion production by plasma membrane NADPH oxidases in different mammalian cell lines (Crane et al. 1994). Noteworthy, changing primary cultures of rat cerebellar granule neurons to a pro-apoptotic low extracellular K^+-medium elicits between 2.5- and 3-fold increase of the level of Cb_5 within 1–2 h, an increase that paralleled the stimulation of superoxide anion production by plasma membrane-associated Cb_5R (Samhan-Arias et al. 2012). In separate studies, we have reported that the Cb_5R isoform 3 (or DIA1) is extensively bound to plasma membrane nanodomains associated with lipid rafts of primary cultures of rat cerebellar granule neurons maturated in vitro (Samhan-Arias et al. 2009; Marques-da-Silva et al. 2010; Marques-da-Silva and Gutierrez-Merino 2014). Moreover, blockade of the plasma membrane NADH oxidase activity in neurons is associated with the inhibition of the superoxide anion production by the flavonoid kaempferol, which also affords a large protection against the generation of oxidative stress and cell death of cerebellar granule neurons in low K^+-pro-apoptotic extracellular medium (Samhan-Arias et al. 2004). In other works, we have shown that administration of kaempferol affords a large protection against rat brain neurodegeneration induced by ischemia–reperfusion following transient middle cerebral artery occlusion (López-Sánchez et al. 2007) or by the neurotoxin 3-nitropropionic acid, an animal model for Huntington's disease (Lagoa et al. 2009). Therefore, the Cb_5R isoform 3/Cb_5 system is emerging as a novel pharmacological target in brain damage induced by ischemia–reperfusion, trauma or brain-related diseases.

In spite of the relevant role of cerebellar granule neurons in interneuronal signaling in the cerebellum cortex, Purkinje cells play the leading role for the integrative response and neuronal output in this brain area. In addition, Purkinje cells neurodegeneration has been reported to mediate the loss of control functions observed in many neurological disorders with cerebellar dysfunction, like cardiac arrest (Paine et al. 2012), spinocerebellar and spastic ataxias (Hourez et al. 2011; Kasumu and Bezprozvanny 2012; Girard et al. 2012), Niemann-Pick type C (Elrick et al. 2010), Huntington's disease (Dougherty et al. 2012) and fetal ethanol neurotoxicity (Dikranian et

al. 2005).

On these grounds, the major aim of this work is the study of the regional and cellular distribution of Cb_5R isoform 3/Cb_5 in the rat cerebellum, as well as in other brain areas, as a logical step towards the identification of neuronal types and structures more prone to neurodegeneration induced by the oxidative stress generated upon deregulation of this redox system.

Materials and methods

Preparation of rat brain slices

The experimental procedures followed the animal care guidelines of the European Communities Council Directive 86/609/EEC. The protocols were approved by the Ethics Committee for Animal Research of the local government.

Male *Wistar* rats 9–10 weeks old, weighing approximately 300 g (n = 8), housed in a 12 h light/dark cycle and with free access to food and water, were used for the histological study. The animals were anesthetized with ketamine (50 μg/g), diazepam (2.5 μg/g) and atropine (0.05 μg/g), and perfused transcardially, first with ice-cold phosphate buffer saline (PBS) and then with 4 % paraformaldehyde in PBS. Brains were removed and immersed in 4 % paraformaldehyde in PBS for post-fixation, dehydrated in a graded series of ethyl alcohol, cleared in xylene, and embedded in paraffin wax, using standard techniques. Afterwards, tissue blocks were cut in coronal Sections (7 μm thick) by a microtome Leica RM2125RT. Slices were deparaffinized with xylene and hydrated with graded series ethanol.

Immunohistochemistry

To identify and localize different cells populations, as well as Cb_5R isoform 3/Cb_5 system, we carried out the following procedures:

Glial fibrillary acidic protein (GFAP), synaptic vesicle protein synaptophysin (SYP), and calbindin immunohistochemistry

For immunohistochemistry, tissue sections were blocked with 1 % bovine serum albumin (BSA) in PBS for 30 min, followed by incubation with 1.5 % normal, goat or horse, serum in 1 % BSA and 0.1 % Triton X-100 for 2 h. Next, slides were incubated, overnight at 4 °C in humidified box, with

primary antibodies (dilution 1:50): (1) mouse anti-GFAP (Sigma: G3893), (2) mouse anti-SYP (Santa Cruz Biotechnology: sc 17750), and (3) goat anti-calbindin D28 K (Santa Cruz Biotechnology: sc 7691). After extensive washing in PBS, sections were again blocked and the secondary antibody (dilution 1:100) was added: goat anti-mouse immunoglobulin G conjugated with alkaline phosphatase (IgG-AP), Santa Cruz Biotechnology: sc 3698, or donkey anti-goat IgG-AP (Santa Cruz Biotechnology: sc 3852), for 3 h at room temperature. Finally, the sections were repeatedly rinsed in PBS, treated with 2 mM levamisole in reaction buffer (100 mM NaCl, 100 mM Tris–HCl pH 9.5, 50 mM $MgCl_2$, 0.25 % Tween-20), revealed with nitroblue tetrazolium/5-bromo-4-chloro-3-indolyl phosphate (NBT/BCIP) supplied by Roche (catalog no. 1681451) in reaction buffer, washed in PBS, dehydrated and mounted in Eukit.

Analysis of the expression levels of Cb_5R isoform 3 and of Cb_5

Western blotting SDS-PAGE were run at a concentration of 12.5 or 15 % acrylamide depending upon the molecular weights of the target proteins, using 2.5 μg of protein of adult rat brain lysates per lane. Gels were transferred to nitrocellulose membranes of 0.2 μm average pore size (Trans-BloT Transfer Medium, BioRad). Nitrocellulose membranes were blocked by 1 h incubation at room temperature with 5 % bovine serum albumin in phosphate-buffered saline with 0.5 % Tween-20 (PBST). Then, nitrocellulose membranes were washed three times with PBST. Immunodetection of Cb_5R isoform 3 and Cb_5 was performed with the primary antibodies used for immunohistochemistry, see below, at a dilution of 1:100 in PBST. After incubation with the primary antibody overnight, membranes were washed six times with PBST and incubated for 1 h at room temperature with the secondary antibody IgG conjugated with horseradish peroxidase (anti-rabbit IgG-peroxidase with a dilution of 1:8000), then washed six times with PBST, followed by incubation for 3 min with SuperSignal West Dura Substrate (Pierce). Western blots were revealed by exposure to an Amersham Hyperfilm MP autoradiography film (GE Healthcare, UK).

Cb_5R isoform 3 and Cb_5 immunohistochemistry For Cb_5R isoform 3 or Cb_5 immunohistochemistry, endogenous peroxidase activity was quenched with 0.5 % H_2O_2 and blocked with 1 % BSA in PBS for 30 min, followed by incubation with 1.5 % normal goat serum in 1 % BSA and 0.1 % Triton X-

100 for 2 h. Next, slides were incubated, overnight at 4 °C in humidified box, with primary antibodies (dilution 1:50): (1) rabbit anti-Cb_5R isoform 3 (anti-DIA1; Protein Tech Group: 10894-1-AP), and (2) rabbit anti-Cb_5 (Santa Cruz Biotechnology: sc 33174). After extensive washing in PBS, sections were again blocked and incubated with the secondary antibody, a biotinylated goat anti-rabbit immunoglobulin G supplied by Vectastain ABC Kit, Vector Laboratories (PK-6101), for 3 h at room temperature. After rinsing in PBS, the sections were incubated with avidin-biotinylated horseradish peroxidase complex (Vectastain ABC Kit) for 30 min at room temperature. Chromogen development was performed with peroxidase substrate solution (Vector VIP substrate, SK-4600). Slides were washed in distilled water, dehydrated and mounted in Eukit.

Additionally, we analyzed a group of brain slides following the same methodology, but using a rabbit anti-neurogranin polyclonal as primary antibody, dilution 1:500 (Chemicon AB5620) to determine the pyramidal cells distribution (Represa et al. 1990).

In all cases, vicinal sections were subjected to Nissl staining (0.1 % cresyl violet in 0.25 % acetic acid) or haematoxylin–eosin (H&E) staining using standard procedures. Sections were digitally photographed in Nikon digital light DS-F1 and Zeiss Axio imager 2 microscope, with camera attached to a dedicated computer compatible with Image-Pro Plus software (Media Cybernetics, Warrendale, PA, USA).

Confocal microscopy Confocal microscopy (Bio-Rad MRC1024 confocal microscope) was performed following the protocol indicated below. Selected slices were blocked with 1 % BSA in PBS for 30 min, followed by incubation with 1.5 % normal sheep serum in 1 % BSA and 0.1 % Triton X-100 for 2 h. Next, slices were split into two groups and incubated, overnight at 4 °C in humidified box, with the following primary antibodies (1:50 dilution): group 1, rabbit anti-Cb_5R isoform 3 (anti-DIA1; Protein Tech Group: 10894-1-AP) and mouse anti-GFAP (Sigma: G3893); group 2, rabbit anti-Cb_5 (Santa Cruz Biotechnology: sc 33174) and mouse anti-GFAP (Sigma: G3893). After extensive washing in PBS, sections were blocked with 1 % BSA in PBS for 30 min, followed by incubation with 1.5 % normal goat serum in 1 % BSA and 0.1 % Triton X-100 for 30 min. Then, blocked sections were incubated with the secondary antibodies, a sheep anti-rabbit IgG-Cy3 (Sigma: C2306) and a goat anti-mouse IgG-Alexa488 (Invitrogen

A11001), dilution 1:100, for 3 h at room temperature. Thereafter, slices were extensively washed in PBS and immediately afterwards observed in the fluorescence microscope. Digital images were captured within 2 h after staining with the secondary antibodies.

In all immunochemistry assays, the lack of staining in controls done with secondary antibody alone, demonstrated the specificity of the primary antibodies staining.

Fluorescence resonance energy transfer (FRET) in cerebellar slices
Following experimental approaches developed in our laboratory (Samhan-Arias et al. 2009; Marques-da-Silva et al. 2010; Samhan-Arias et al. 2012; Marques-da-Silva and Gutierrez-Merino 2012), we analyzed the staining pattern of Cb_5R isoform 3 and cholera toxin subunit B (CTB, a lipid rafts marker; Janes et al. 1999; O'Connell et al. 2004) and FRET between donor–acceptor dyes bound to both proteins.

Slices were blocked with 1 % BSA in PBS for 30 min, followed by incubation with 1.5 % normal sheep serum in 1 % BSA and 0.1 % Triton X-100 for 2 h. Next, slices were incubated, overnight at 4 °C in humidified box, with the primary antibody rabbit anti-Cb_5R isoform 3 (Protein Tech Group: 10894-1-AP) dilution 1:50. After extensive washing in PBS, sections were again blocked and incubated with the secondary antibody, a sheep anti-rabbit IgG-Cy3 (Sigma: C2306), dilution 1:100, for 3 h at room temperature. For controls of single staining with CTB-Alexa488, the tissue sections were subjected to the same treatments using rabbit-IgG (Invitrogen Z25305) instead of the primary antibody for Cb_5R. Thereafter, slices were extensively washed in PBS and immediately afterwards observed in the fluorescence microscope. Slices stained with anti-Cb_5R isoform 3/IgG-Cy3 were subsequently stained with 0.2 μg CTB-Alexa488 (Invitrogen: C22841) in PBS plus 0.2 % Triton X-100, for 1 h at room temperature and later washed with PBS. Digital images were captured within 2 h after staining with the IgG-Cy3 secondary antibody.

For FRET imaging, quantitative green and red fluorescence intensity images were acquired with fixed exposure times using the OrcaR2-digital camera and HCImage software attached to our epifluorescence Nikon Diaphot 300 microscope with an excitation filter of 470 nm and dichroic mirror/emission filters of 510/520 nm (green fluorescence) and 580/590 nm (red

fluorescence).

Results and discussion

In this work, we have studied the regional and cellular distribution of the redox Cb_5R isoform 3/Cb_5 system in the adult rat brain by immunocytochemistry, with more detail in the cerebellum cortex which was found to display the highest level of expression of this system. First, we selected antibodies displaying a high specificity for Cb_5R isoform 3 and for Cb_5 in adult rat brain lysates by Western blotting (Supplementary Figure S1), after screening several commercially available antibodies against these proteins. Rabbit anti-Cb_5R isoform 3 (or anti-DIA1; Protein Tech Group: 10894-1-AP) gave a single immunoreactive band in adult rat brain lysates, with the expected molecular weight for Cb_5R isoform 3 (Supplementary Figure S1A). Rabbit anti-Cb_5 (Santa Cruz Biotechnology: sc 33174) gave immunoreactive bands of molecular weights corresponding to monomers, dimmers and trimers of Cb_5 (Supplementary Figure S1B), as expected for a protein expressing two major isoforms (soluble and membrane-bound) (Samhan-Arias and Gutierrez-Merino 2014b) and which has been shown to form homomeric aggregates in living cells (Storbeck et al. 2012). On these grounds, these were the primary antibodies chosen for immunohistochemistry of adult rat brain slices.

Because the redox Cb_5R isoform 3/Cb_5 system has shown to play a major role in oxidative stress-mediated apoptosis of cerebellar neurons maturated in culture in vitro (Samhan-Arias et al. 2009, 2012), we describe first the regional and cellular distribution of this enzymatic complex in cerebellum by immunocytochemistry.

Regionalization of Cb_5R isoform 3 and Cb_5 expression in adult rat cerebellum cortex

Our results showed (Fig. 1) that Cb_5R isoform 3 is more highly enriched at the granular than at the molecular layer in the cerebellum cortex (Fig. 1a–c), while Cb_5 staining shows a more diffuse distribution in these two layers (Fig. 1d–f). Controls done with the primary antibodies replaced by rabbit IgG and later treated with the secondary antibody used for the immunohistochemistry images (biotinylated goat anti-rabbit IgG) or with the secondary antibody alone showed lack of significant staining with biotinylated goat anti-rabbit IgG when compared with the staining observed

after immunohistochemistry with anti-Cb_5R isoform 3 and anti-Cb_5 (*data not shown* or supplementary Figure S2). In addition, a significant signal of Cb_5R isoform 3 and Cb_5 staining was found between the granular and molecular areas, at the corresponding location of the Purkinje cells layer. As expected, we found that both anti-Cb_5R isoform 3 and anti-Cb_5 also heavily stained the cerebellum vascularity and particularly the capillary network linked to the *piamater* (Fig. 1c, f). These results are consistent with the well-marked expression of the Cb_5R/Cb_5 system in erythrocytes, which is known to catalyze most of the methemoglobin reductase activity of erythrocytes (Hultquist and Passon 1971; Leroux et al. 1975; Vieira et al. 1995; Aalfs et al. 2000), and also in endothelial cells (Chatenay-Rivauday et al. 2004).

Fig. 1

Light micrographs of coronal sections at cerebellar and brain stem level after immunohistochemistry with anti-Cb_5R isoform 3 (**a**), anti-Cb_5 (**d**), anti-GFAP (**g**) and anti-SYP (**j**) antibodies. In cerebellar cortex, anti-Cb_5R isoform 3 (**a**, **b**) and anti-GFAP (**g**, **h**) mark mainly the granular layer (gl), while anti-Cb_5 (**d**, **e**) and anti-SYP (**j**, **k**) display a higher expression level in the molecular layer (ml). Purkinje cell layer (pcl) is marked with anti-Cb_5R isoform 3 (**c**) and anti-Cb_5 (**f**). Additionally, cerebellum vascularity (*arrows*) is also observed (**c**, **f**), particularly linked to the piamater (*asterisks*). Note at brain stem level the high expression levels of Cb_5R isoform 3 (**a**) in lateral vestibular (LVe) and motor trigeminal (Mo5) nuclei, among others

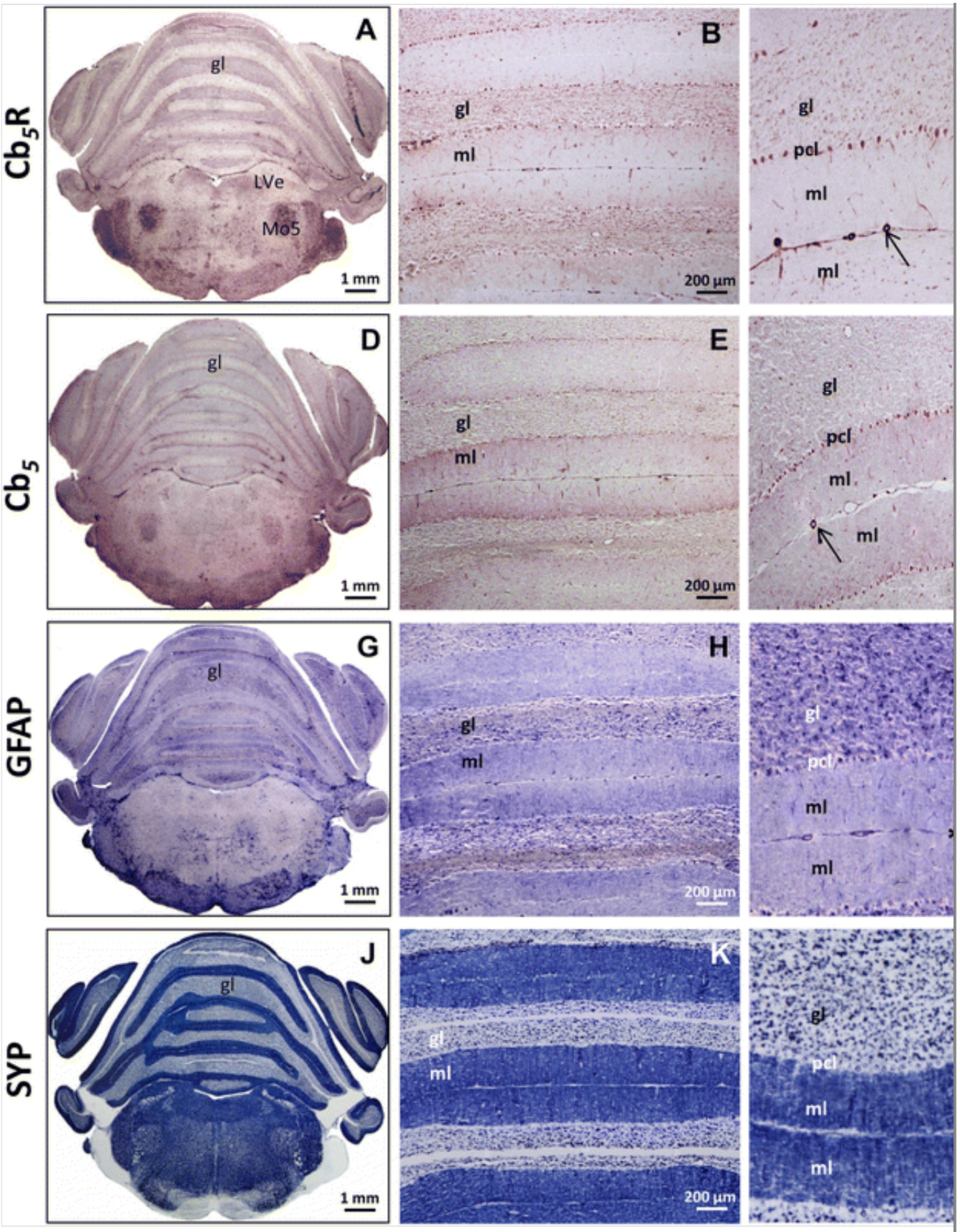

Aiming to improve the regionalization and cellular distribution of Cb_5R isoform 3 and Cb_5 within rat cerebellum slices, vicinal sections were stained with anti-GFAP (Fig. 1g–i), an astrocyte and a glial marker (Nakamura and Uchihara 2004; Taft et al. 2005; Roda et al. 2008), and anti-SYP (Fig. 1j–l), specifically associated with synapses linked to vesicle secretion (Fujita et

al. 1996; Nakamura and Uchihara 2004). Our results showed staining of granular and molecular layers in the cerebellum cortex with both antibodies. However, anti-GFAP antibody stained mainly the granular layer (Fig. 1h), while anti-SYP displayed a higher intensity of staining in the molecular layer (Fig. 1k). Although this regionalization is similar for Cb_5R isoform 3 and Cb_5 staining, respectively, a more detailed observation of the images (Fig. 1c, f, i, l) revealed that cellular distribution did not appear strictly coincident. To further assess experimentally that both Cb_5R isoform 3 and Cb_5 were largely enriched in neuronal bodies at the granular layer, we have acquired confocal microscopy images with double staining with anti-Cb_5R isoform 3 and anti-GFAP (Fig. 2a) and with anti-Cb_5 and anti-GFAP (Fig. 2b). The results clearly demonstrated that the cells displaying high-intensity labeling with anti-Cb_5R isoform 3, or with anti-Cb_5, are not the glial cells and astrocytes, heavily labeled with anti-GFAP.

Fig. 2

Confocal microscopy images of the cerebellar cortex double stained with anti-GFAP (*green channel*) and anti-Cb_5R isoform 3 or anti-Cb_5 (*red channel*) antibodies. **a** Confocal microscopy image of the cerebellar cortex double stained with anti-GFAP (*green*) and anti-Cb_5R isoform 3 (*red*). **b** Confocal microscopy image of the cerebellar cortex double stained with anti-GFAP (*green*) and anti-Cb_5 (*red*). The images revealed that the cellular bodies most heavily stained with anti-Cb_5R isoform 3 and with anti-Cb_5 are not the cellular bodies stained by anti-GFAP (glial cells and astrocytes). *gl* granular layer, *pcl* Purkinje cell layer, *ml* molecular layer

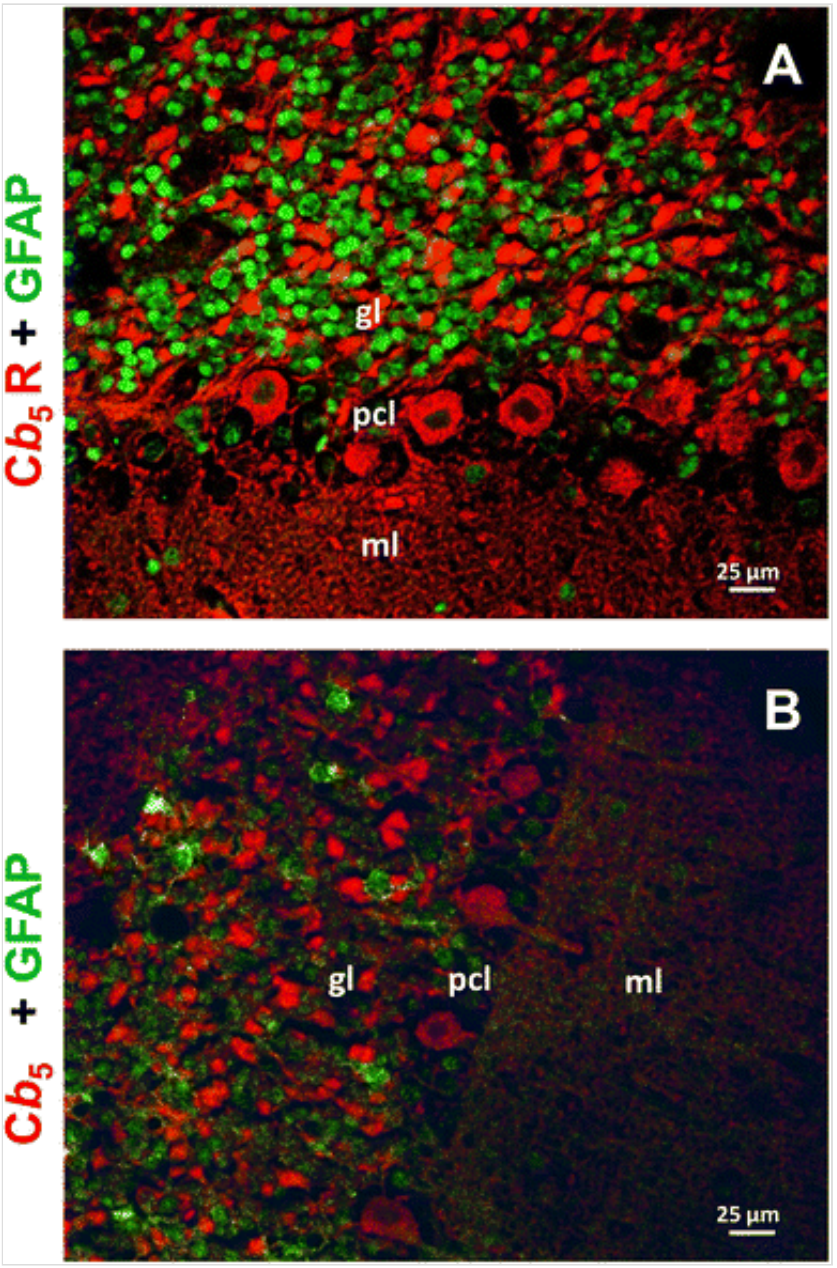

To gain a deeper insight into Cb_5R isoform 3 and Cb_5 regionalization in the granular layer, cerebellum slides were subjected to the Nissl staining procedure (Pilati et al. 2008), which labels the endoplasmic reticulum, mainly associated with somas in neurons within this layer (Fig. 3). Nissl and anti-Cb_5R isoform 3 staining displayed a strong labeling pattern of the neuronal soma of the granular layer, as well as the area corresponding to Purkinje cell layer (Fig. 3e, f), being weaker with anti-Cb_5 (Fig. 3h, i). Again, controls done with the primary antibodies replaced with rabbit IgG and later treated with the secondary antibody used for the immunohistochemistry images (biotinylated goat anti-rabbit IgG) or with the secondary antibody alone showed lack of significant staining with biotinylated goat anti-rabbit IgG when compared with the staining observed after immunohistochemistry with anti-Cb_5R isoform 3 and anti-Cb_5 (*data not shown* or supplementary Figure S2). This is in good agreement with the well-

known predominant subcellular localization of Cb_5R in the endoplasmic reticulum of mammalian cells (Borgese et al. 1993). However, while the Nissl staining displayed a characteristic round or spheroid shape, as expected for the widespread structure of endoplasmic reticulum surrounding the large nuclei of cerebellar neurons, the anti-Cb_5R isoform 3 staining revealed a more irregular and diffuse peripheral morphology, which is consistent with the association of the Cb_5R isoform 3 with lipid microdomains rafts of the plasma membrane (Chatenay-Rivauday et al. 2004; Samhan-Arias et al. 2009; Marques-da-Silva et al. 2010; Samhan-Arias et al. 2012). This hypothesis can only be experimentally demonstrated using FRET, and deserved to be experimentally assessed because in previous studies, we showed that the Cb_5R isoform 3 pool which is associated with lipid rafts of the plasma membrane of cerebellar granule neurons, i.e., within FRET distance of cholera toxin B binding sites, is the Cb_5R involved in the generation of the neuronal death caused by oxidative stress (Samhan-Arias et al. 2009, 2012). To experimentally assess this point, we have performed FRET imaging using cerebellar slices stained with fluorescent cholera toxin B, a widely used marker for lipid rafts (Janes et al. 1999; O'Connell et al. 2004).

Fig. 3

Light micrographs of coronal sections at cerebellar and brain stem level after Nissl staining (**a**, **b**, **c**) and immunohistochemistry with anti-Cb_5R isoform 3 (**d**, **e**, **f**) and anti-Cb_5 (**g**, **h**, **i**) antibodies. The abbreviations gl, pcl and ml have the meaning indicated in the legend for the Fig. 2. Nissl staining and anti-Cb_5R isoform 3 labeled most of cells from the granular (gl) and Purkinje cell (pcl) layers, while labeling is less intense with anti-Cb_5. Selected regions are shown with higher magnification in panels **c**, **f** and **i** to highlight the labeling of the dendritic trunk of Purkinje cells by anti-Cb_5R isoform 3 and also by anti-Cb_5 (marked by *arrows*), although less intense in this latter case

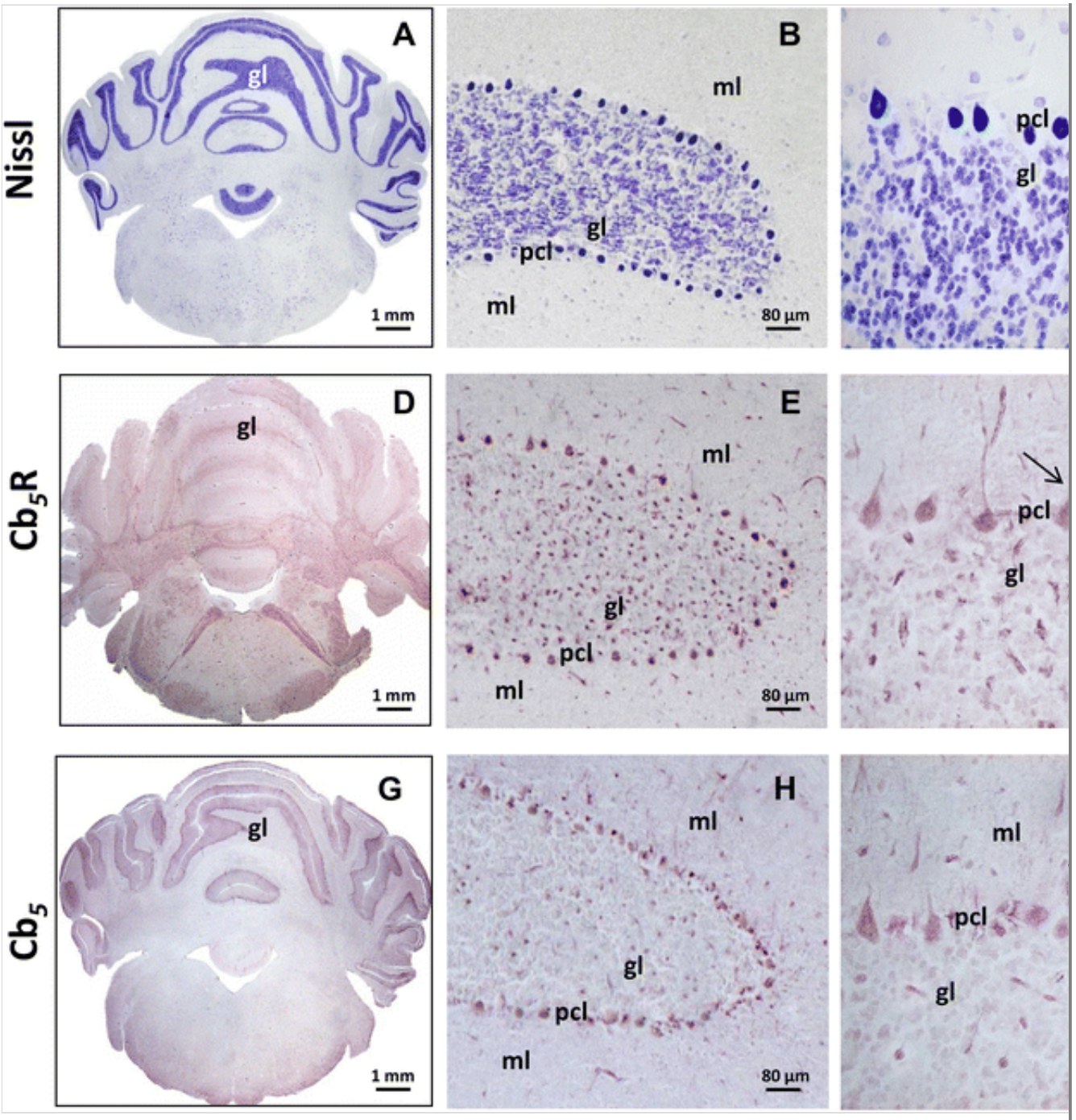

AQ1

Using quantitative fluorescence microscopy imaging, we have observed that the staining of cerebellar slices with the Alexa488-fluorescent cholera toxin B preferentially labeled the granular over the molecular layer (Fig. 4a, green fluorescence). It is to mention that the Purkinje cells layer displayed lower intensity of fluorescent cholera toxin B labeling. These findings are consistent with the presence of a high-density network of lipid rafts in the plasma membrane of the soma of cerebellar granule neurons, as noticed in our previous work carried out with these neurons matured in vitro (Samhan-Arias et al. 2009). As for FRET experiments, we have used Alexa488-cholera toxin B as donor and the complex anti-Cb_5R isoform 3/IgG-Cy3 as

acceptor, before performing the double labeling of cerebellar slices with Alexa488-cholera toxin B and anti-Cb_5R isoform 3/IgG-Cy3, the following green and red fluorescence images were acquired as controls taken with the same exposure times and instrument setup: images of non-stained slices, images of slices treated with IgG-Cy3 in the absence of preincubation with anti-Cb_5R, and images of slices after single labeling with Alexa488-cholera toxin B or with anti-Cb_5R isoform 3/IgG-Cy3. Black images like those shown for green and red fluorescence of slices stained only with anti-Cb_5R isoform 3/IgG-Cy3 in the Fig. 4a were also obtained for non-stained slices and for slices treated with IgG-Cy3 in the absence of preincubation with anti-Cb_5R. These results allowed us to conclude: (1) under our conditions for fluorescence microscopy images acquisition, the autofluorescence of cerebellar slices is negligible, (2) the treatment of slices only with the secondary fluorescent conjugated IgG-Cy3 antibody did not produce a significant fluorescence background signal, and (3) both the green and red fluorescence intensity of slices stained with anti-Cb_5R isoform 3/IgG-Cy3 only are negligible (shown in the Fig. 4a). Thus, the large increase of red fluorescence upon double labeling of cerebellar slices with anti-Cb_5R isoform 3/IgG-Cy3 and Alexa488-cholera toxin B shown in Fig. 4a revealed the occurrence of FRET between Alexa488 (FRET donor) and Cy3 (FRET acceptor). Merge images (Fig. 4b) illustrate the increase in ratio between red and green fluorescence intensity (areas in orange) in the Purkinje cells soma, thereby monitoring also the FRET occurrence in these neurons.

Fig. 4

A large pool of Cb_5R isoform 3 is associated with lipid rafts microdomains in Purkinje and cerebellar granule neurons in the cerebellum cortex. **a** Part of Cb_5R isoform 3 expressed in the cerebellar cortex is within FRET distance with cholera toxin binding sites. Representative quantitative fluorescence microscopy images of 7 μm-thick cerebellar slices stained with the Alexa488 fluorescent-conjugate of cholera toxin B (CTB-A488) and Cb_5R isoform 3 tagged with IgG-Cy3 (Cb_5R*Cy3). *Green* F and *Red* F mean *green* and *red* fluorescence intensity images, respectively; gl and ml mark granular and molecular layers, respectively. **b** *Yellow-orange* stained areas in the merge *red*/*green* images also highlighted the areas of co-localization of CTB and Cb_5R isoform 3 in cerebellar slices stained with CTB-A488 as fluorescence donor and Cb_5R*Cy3 as fluorescence acceptor. In these images, pcl, gl and ml mark Purkinje cells, granular and molecular layers, respectively

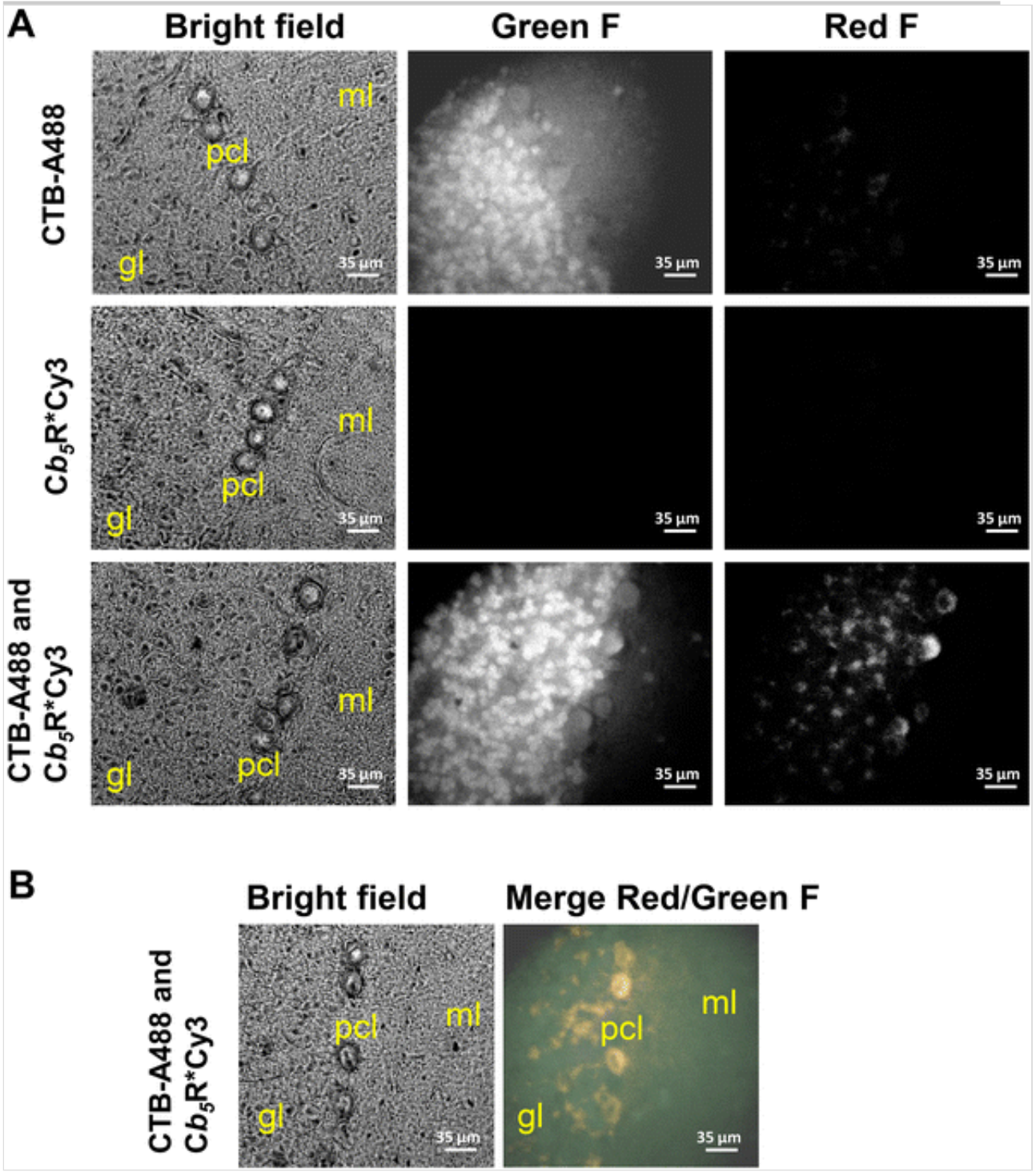

To further assess the identification of these neurons as Purkinje cells, we also used calbindin D28 K antibody, known as a Purkinje cells marker (Celio 1990; Dusart et al. 1997). As mentioned above (Fig. 1), after staining with anti-Cb_5R isoform 3 antibody, we observed large neuronal somas aligned between the granular and molecular layers. Their location, size and morphology strongly suggested a high expression level of Cb_5R in Purkinje cells. To further assess this important point, we acquired images of slices stained with anti-calbindin D28 K (Fig. 5a), which is a characteristic marker of Purkinje cells. The comparison of the images stained with anti-calbindin D28 K with those obtained using anti-Cb_5R isoform 3 and anti-Cb_5 staining

(Figs. 5b, c) allowed us to conclude that Purkinje cells express both proteins at levels much higher than other cells present in the cerebellar cortex.

Fig. 5

Light micrographs of cerebellar cortex after immunohistochemistry with anti-calbindin (**a**), anti-Cb_5R isoform 3 (**b**), anti-Cb_5 (**c**) and anti-GFAP (**d**) antibodies. Note the Purkinje cell bodies (*asterisks*) labeled with anti-Cb_5R isoform 3, anti-calbindin and anti-Cb_5 in the Purkinje cell layer (pcl). Anti-calbindin also marks the numerous dendrite extensions of Purkinje cells in the molecular (ml) and the axons in the granular (gl) layers. Anti-Cb_5 and anti-GFAP mark the Bergman glial cells network of connections (*arrowheads*) in the molecular layer (ml) and body (*arrows*) in the Purkinje cell layer (pcl)

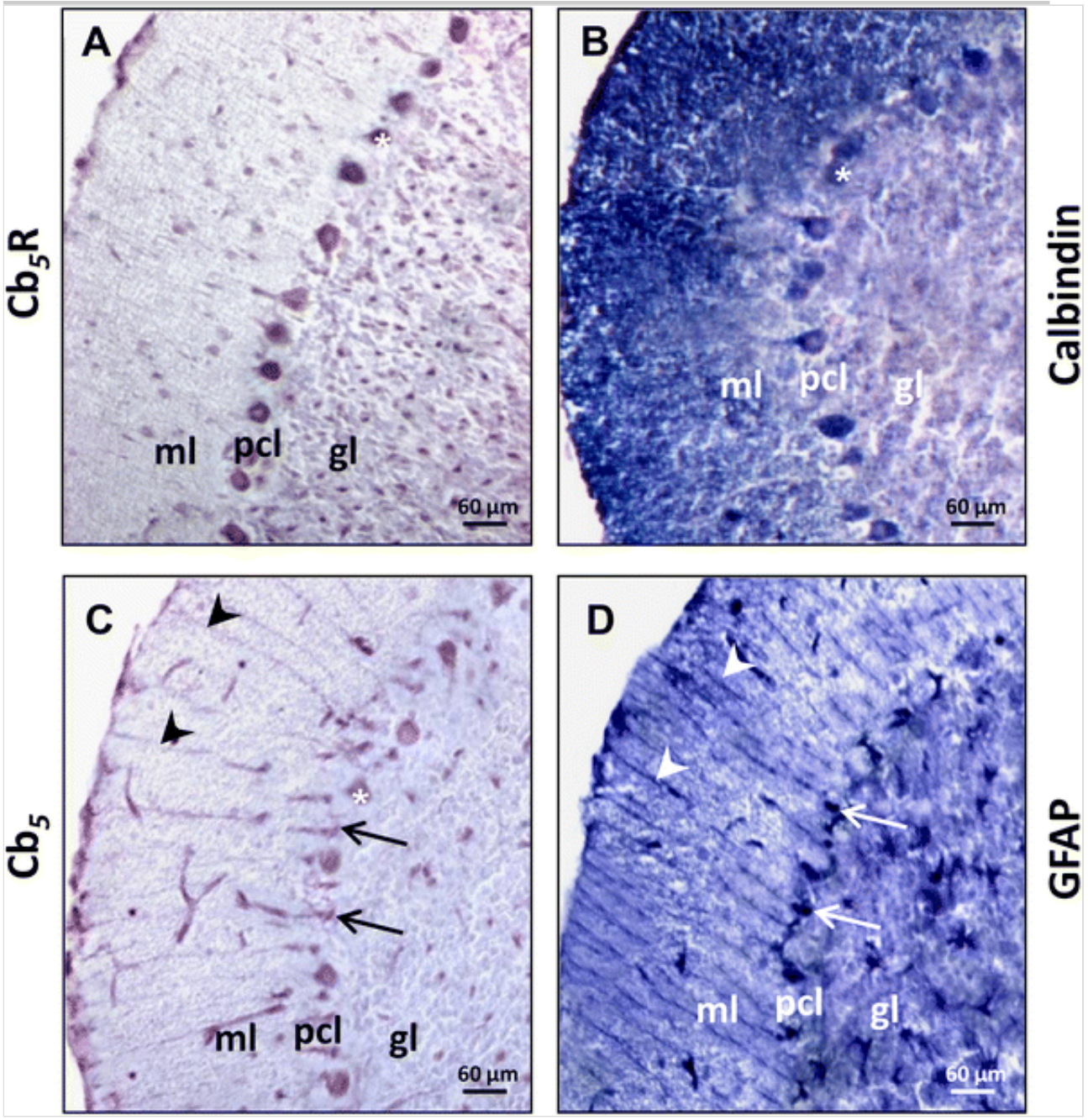

Finally, we observed a more widespread distribution of Cb_5, mainly at the molecular layer, and a distribution pattern which pointed out staining of a network of connecting structures located among Purkinje cells (Fig. 5c). As Bergmann glial cells modulate Purkinje cells via Ca^{2+}-dependent K^+ channels (Wang et al. 2012), establishing the fine motor coordination (Saab et al. 2012), we also performed staining with anti-GFAP (Fig. 5d), a specific Bergman cells marker (O'Callagan 1988; Nakamura and Uchihara 2004; Roda et al. 2008). These results strongly suggested that anti-Cb_5 heavily stains also the bodies and connections of Bergmann glial cells surrounding the soma of Purkinje neurons.

All these results revealed that, although the Cb_5R isoform 3 level of expression is weaker in the molecular layer, Cb_5 antibody highly marks this layer, in particular at the level of the network of Bergman glial cells connections, as revealed by anti-GFAP antibody staining. Moreover, the high levels of SYP expression indicated a large number of synaptic connections, a characteristic of the multiple Purkinje cells dendritic structures, identified by a specific antibody against the Purkinje cell marker calbindin-D28 K. Furthermore, Purkinje cell somas located between the molecular and granular layers are heavily stained with anti-calbindin-D28 K and displayed also a high staining with anti-Cb_5R isoform 3 and anti-Cb_5. Finally, at the level of the granular layer, anti-Cb_5R isoform 3 staining closely matches Nissl staining of the granular cells and anti-Cb_5 staining, despite being less intense, also showed a staining pattern close to that observed for anti-Cb_5R isoform 3 staining. Also, this layer contains the Purkinje axonal prolongations and its recurrent collateral branch, supported by calbindin D28 K and SYP staining. Taking in account all these data, our results suggested that the Cb_5R isoform 3/Cb_5 enzyme complex is heavily expressed in neurons that plays a major role in the control of efferent connections in the cerebellar cortex, due to the high expression levels of both proteins at the regions involved in the neuronal output modulation.

Cb_5R isoform 3 and Cb_5 are highly expressed in brain stem motor nuclei

It is well known that the axon of a Purkinje cell leaves the inner pole of the soma, crosses the granular layer and enters the underlying white matter. These projections of the Purkinje cells are also stained with anti-Cb_5R isoform 3, anti-Cb_5 and anti-calbindin (Fig. 6), and reach the vestibular and

cerebellar nuclei, where we found that Cb_5R isoform 3 is also highly expressed (Figs. 7, 8). The efferent cerebellar connections end in the brain stem nuclei (Stephenson and Kushner 1988), an area that showed high levels of Cb_5R isoform 3 staining as well. In particular, we observed heavy staining in motor trigeminal nucleus, hypoglossal nucleus, dorsal motor nucleus of the vagus nerve, spinal nucleus of the trigeminal, ventral cochlear nucleus and facial nerve (root of facial nerve), among others (Figs. 7, 8, 9).

Fig. 6

Light micrographs of cerebellar sections after immunohistochemistry with anti-calbindin (**a**, **b**), anti-Cb_5R isoform 3 (**c**, **d**) and anti-Cb_5 (**e**, **f**) antibodies. The images shown in the panels **b**, **d** and **f** are magnifications of the areas labeled with a large *square in panels* **a**, **c** and **e**, respectively. Note the reaction of Purkinje cell axons (*arrowheads*) with the three antibodies at the level of the cerebellar white matter (wm). *ml* molecular layer. *gl* granular layer

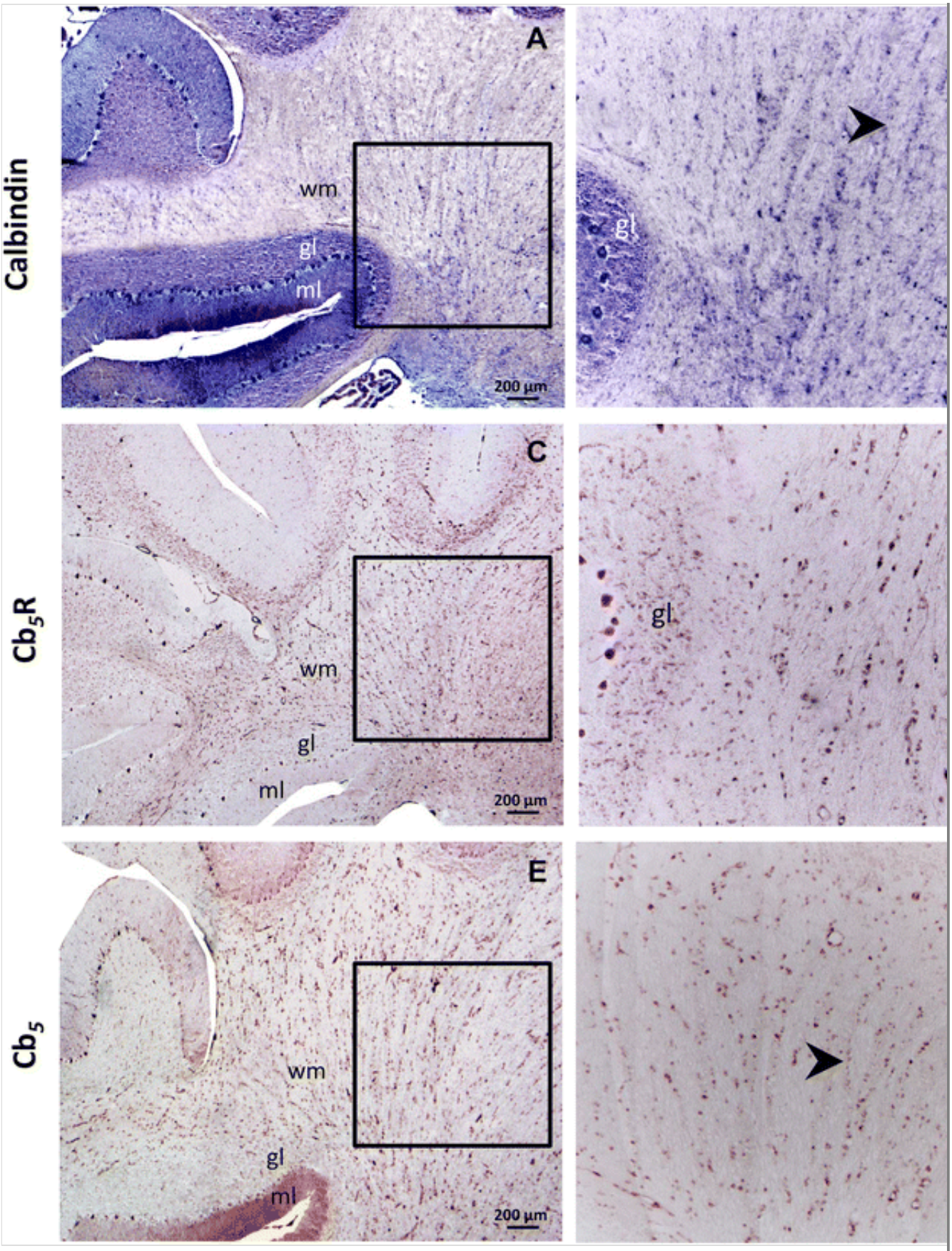

Fig. 7

Light micrographs of coronal sections at brain stem level (*pons*) after immunohistochemistry with anti-Cb_5R isoform 3 antibody. Note the reaction (**a**) in the large neurons (**b**) of the lateral vestibular nucleus (LVe) and the large multipolar neurons interposed with the smaller multipolar cells (**c**) of the motor

trigeminal nucleus (Mo5). A more caudal section (**d**) shows the ascending fibers of the facial nerve (asc7) labeled with anti-Cb_5R isoform 3. *PnC* pontine reticular caudal nucleus, *VCo* ventral cochlear nucleus, *py* pyramidal tract, *7n* facial nerve (root of facial nerve), *4V* fourth ventricle

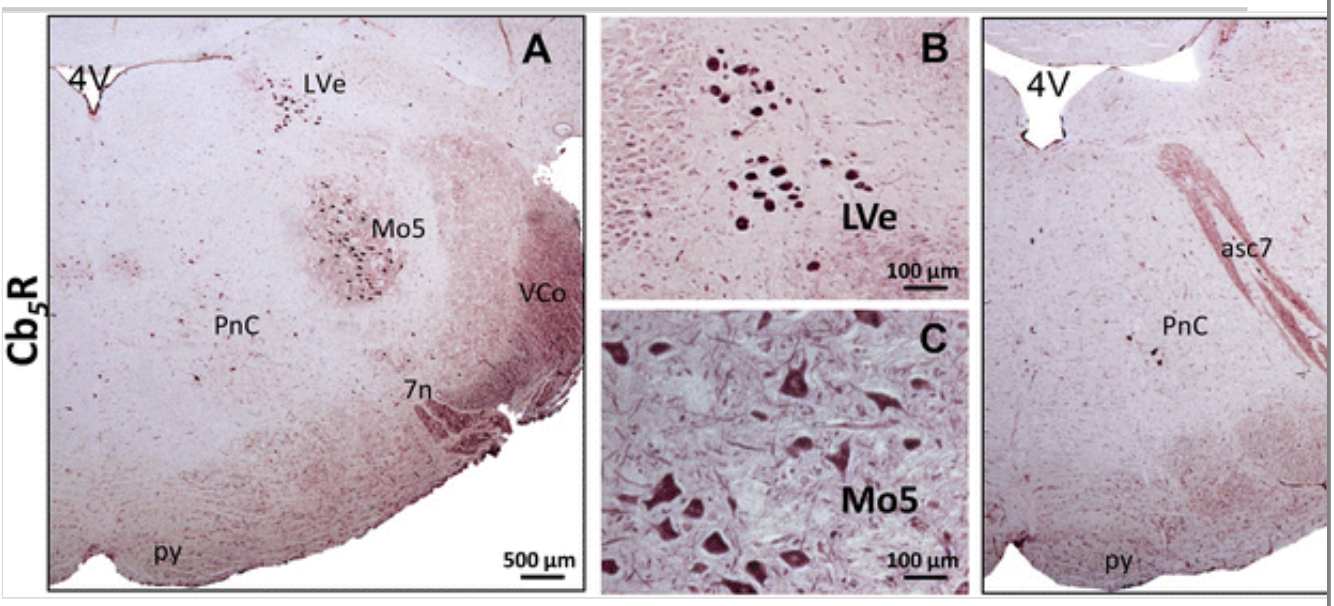

Fig. 8

Light micrographs of coronal sections at cerebellar and brain stem level after immunohistochemistry with anti-SYP (**a**) and anti-Cb_5R isoform 3 (**b**–**d**) antibodies. Note the reaction in the fastigial (FN), interposed (IP) and dentate (DN) cerebellar nuclei (**a**, **b**). Anti-Cb_5R isoform 3 marks the neurons of the nucleus spinal tract trigeminal nerve (oral) (Sp5O), as well as the spinal vestibular (SpVe) and gigantocellular reticular (Gi) nuclei, among others (**b**). Note the reaction of anti-SYP (**a**) and anti-Cb_5R isoform 3 (**b**) in the complex cyto-architecture within the ventral cochlear nucleus (VCo), which contains many neuronal types with distinct dendritic field characteristics. Higher magnification shows the somas in spinal vestibular nucleus (**c**) and large multipolar neurons in gigantocellular reticular nucleus (**d**). *py* pyramidal tract, *4V* fourth ventricle

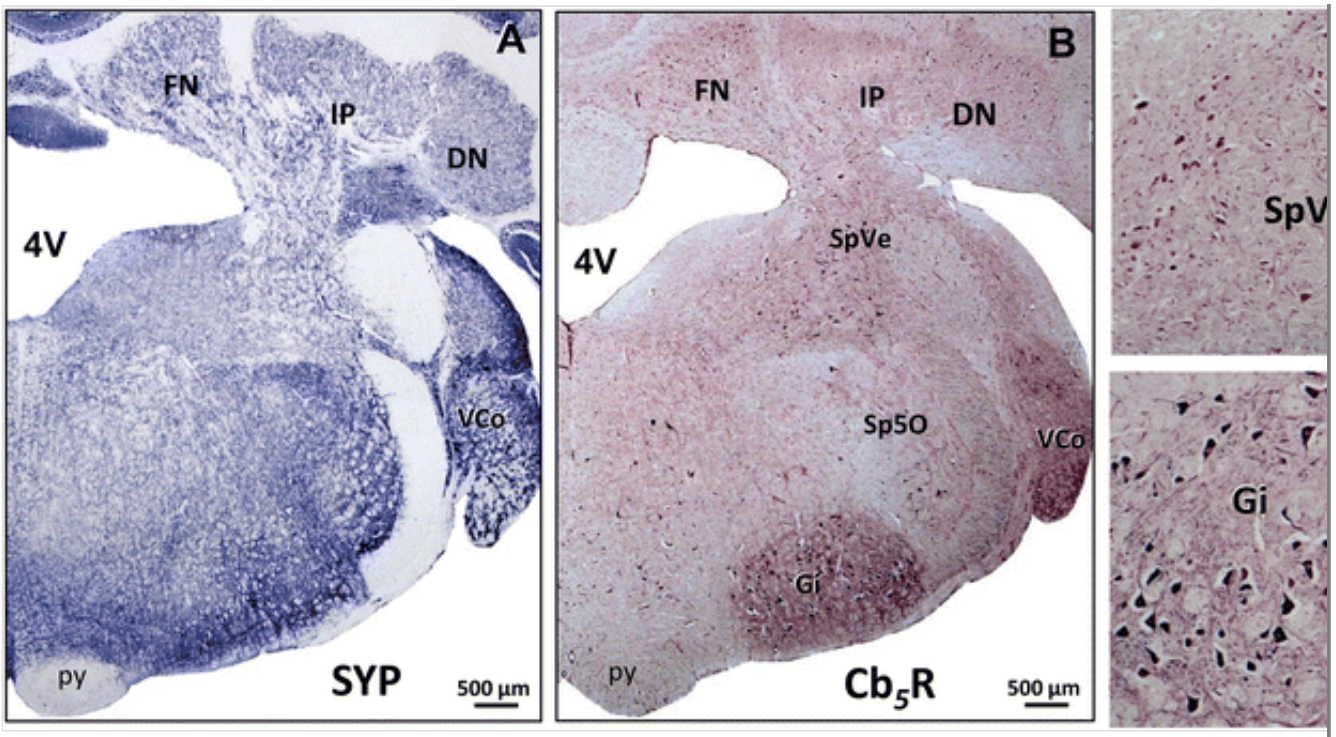

Fig. 9

Light micrographs of a coronal section at *medulla oblongata* level after immunohistochemistry with anti-Cb_5R isoform 3 antibody. Note the reaction in solitary tract (*Sol*), dorsal motor of vagus (*X*), hypoglossal (*XII*), spinal tract trigeminal nerve (oral) (Sp5O), parvocellular reticular (*PcRt*), ambiguus (*Amb*) and lateral reticular (*LRt*) nuclei, among others. Higher magnification shows a detail of these structures: *Sol*, *X*, *XII*, and *PcRt* (**b**), as well as the somas in *LRt* and large motor neurons in Amb (**b**). *py* pyramidal tract, *4V* fourth ventricle

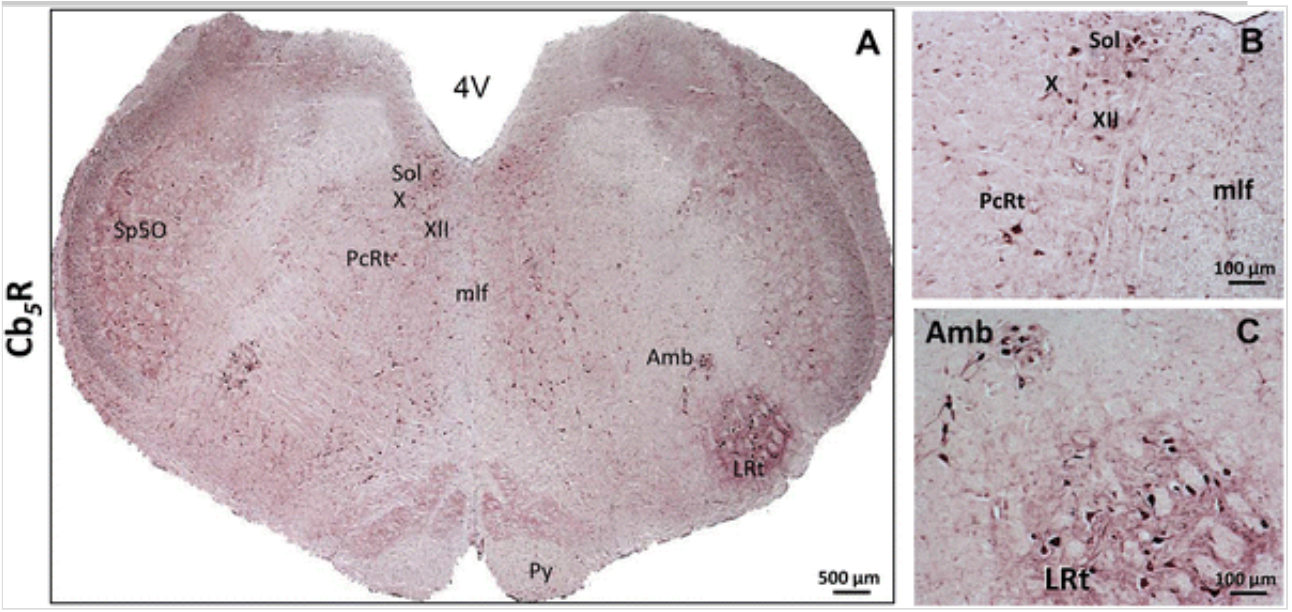

Reticular formation receives precise information from the cerebellar nuclei,

mainly the fastigial nucleus. A detail of more amplification highlighted the enrichment of Cb_5R isoform 3 in neuronal soma of caudal pontine reticular nucleus (Fig. 8), which is composed by gigantocellular neurons (Fig. 8d) controlling involuntary movements associated with mastication and grinding of teeth during sleep (Sasaki et al. 2004). Thus, the high level of Cb_5R isoform 3 found in caudal pontine reticular nucleus correlates well with the generalized dystonia and movements disorders noticed in patients suffering type II-recessive congenital methemoglobinemia (Leroux et al. 1975; Toelle et al. 2004; Percy and Lappin 2008; Ewenczyk et al. 2008; Huang et al. 2012).

Cb$_5$R isoform 3 and Cb$_5$ are also highly expressed in cerebral neocortex and hippocampus

The high levels of Cb_5R isoform 3 expression in pyramidal neurons belonging to motor nuclei of the brain stem prompted us to extend our studies to other areas of the brain intimately connected with the functional control and coordination of voluntary and involuntary movements, such as the primary and secondary motor areas of the frontoparietal cerebral cortex and the hippocampus. Large pyramidal neurons of these areas of the cerebral cortex and hippocampus displayed an expression level of Cb_5R isoform 3 and Cb_5 higher than other cells in these brain regions (Figs. 10, 11). Controls done with the secondary antibody used for the immunohistochemistry images (biotinylated goat anti-rabbit IgG) alone showed lack of significant staining with biotinylated goat anti-rabbit IgG when compared with the staining observed after immunohistochemistry with anti-Cb_5R isoform 3 and anti-Cb_5 (*data not shown* or supplementary Figure S2). We analyzed the staining pattern obtained with anti-Cb_5R isoform 3 and anti-Cb_5 in comparison with neurogranin immunostaining, which has been described as a pyramidal neuron marker (Represa et al. 1990). Our results pointed out that Cb_5R isoform 3, Cb_5 and neurogranin showed a similar staining pattern in cerebral neocortex, in pyramidal soma and dendritic trees. Observation with higher magnification of the rat brain primary and secondary motor areas of the frontoparietal neocortex revealed a heavy staining of pyramidal neurons with anti-Cb_5R isoform 3 and also with anti-Cb_5 (Fig. 10, images of c and d columns). The high level of expression of Cb_5R isoform 3 and Cb_5 in giant pyramidal neurons of the primary motor areas (Betz cells) has a special integrative relevance in this work, as these neurons are known to have very long axons which form synapses with neurons of the brain stem motor nuclei

mentioned above.

Fig. 10

Light micrographs of coronal brain sections after H&E staining and immunohistochemistry with anti-Cb_5R isoform 3, anti-Cb$_5$ and anti-neurogranin antibodies: motor areas of the rat cerebral cortex. In column **a**, a trapezoid drawn in black marks the motor areas of the cerebral cortex of a frontoparietal brain slice that are shown with higher detail in columns **b**, **c** and **d**. Column **b** shows low resolution images of the layers *I–V* of the primary and secondary motor areas of the rat cerebral cortex (MOp and MOs, respectively). Column **c** shows higher magnification images of the *V* layer of the primary motor area (MOp) that revealed the heavy staining of the soma of giant pyramidal neurons with anti-Cb_5R isoform 3 and with anti-Cb_5. Column **d** shows higher magnification images of the II-III layer of the secondary motor area (MOs) that also revealed the heavy staining of the soma of pyramidal neurons of this layer with anti-Cb_5R isoform 3 and with anti-Cb_5

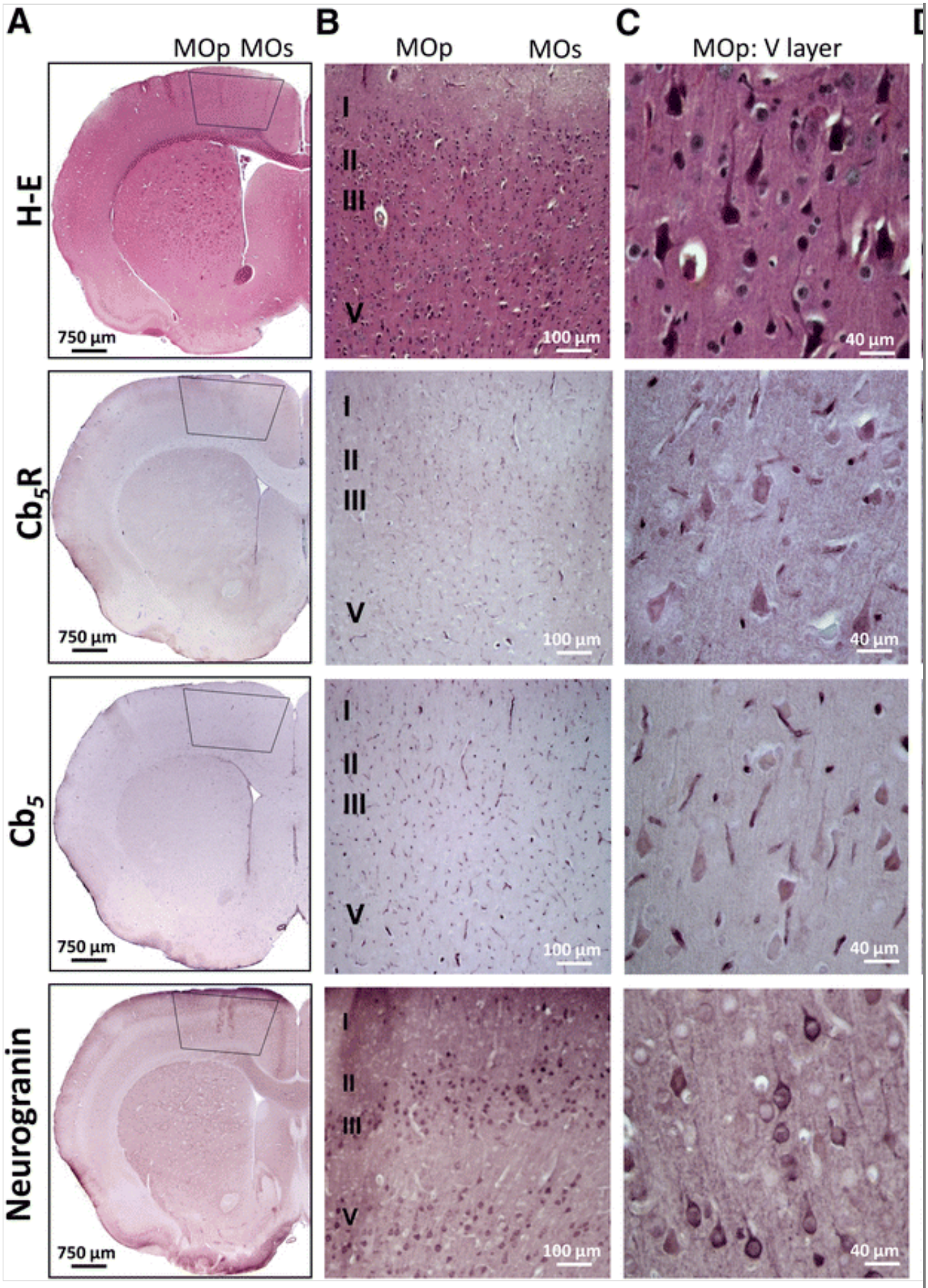

Fig. 11

Light micrographs of coronal brain sections after H&E staining and immunohistochemistry with anti-Cb_5R isoform 3, anti-Cb$_5$ and anti-

neurogranin antibodies: hippocampus. In column **a**, the abbreviation Hip marks the hippocampal areas of a frontoparietal brain slice that are shown with higher magnifications in columns **b**, **c** and **d**. Column **b** shows microscopy images acquired with a magnification suitable to visualize the overall morphology of the Ammon's horn. Column **c** shows microscopy images of hippocampal CA1 pyramidal field acquired with an intermediate magnification and column **d** shows microscopy images with a higher magnification for a better visualization of the soma of CA1 pyramidal neurons. The soma of pyramidal cells were stained: p, pyramidal layer; o, *stratum oriens*; ra, *stratum radiatum*

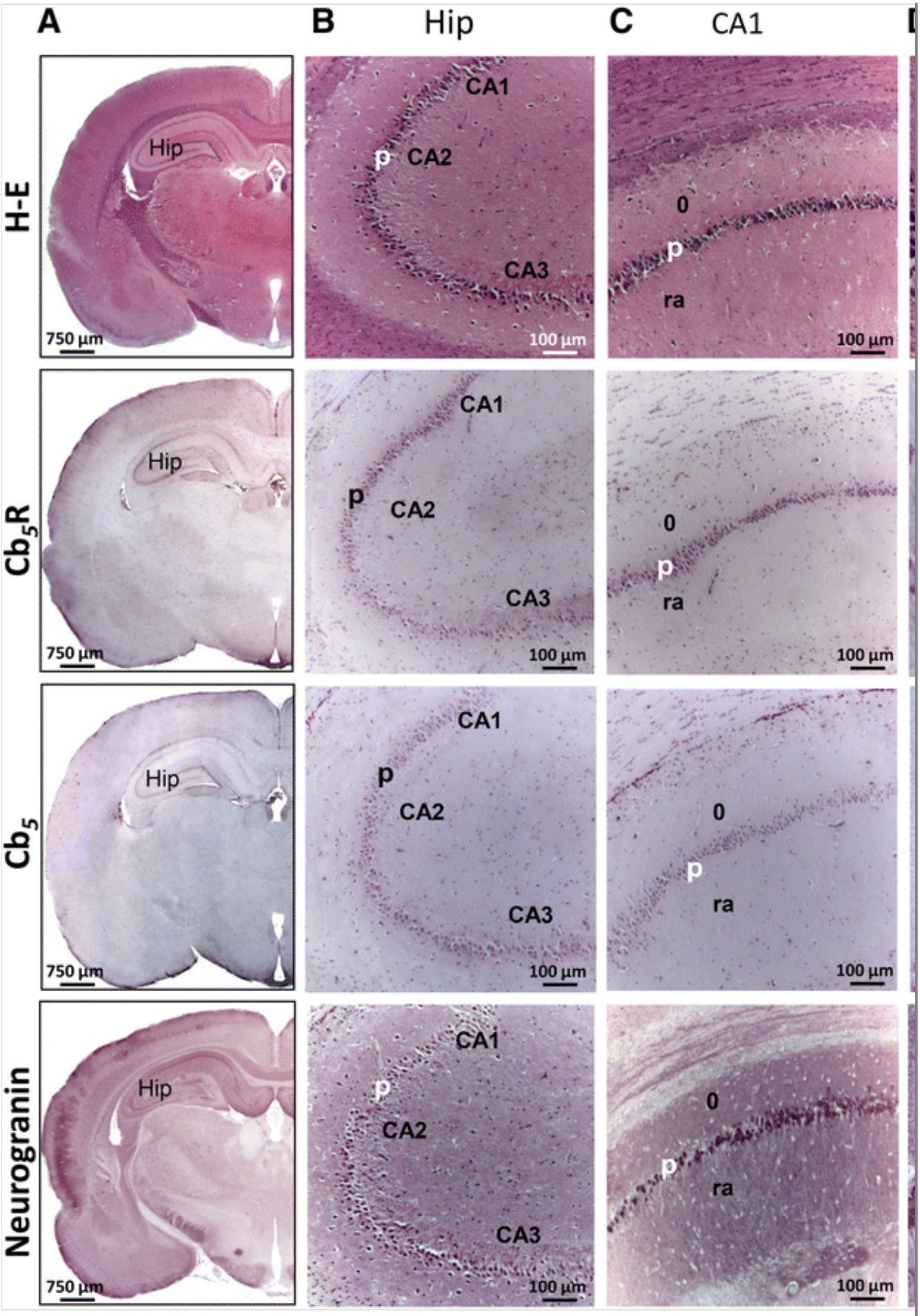

Within the hypocampal complex, pyramidal neurons of Ammon´s horn and in particular CA1 pyramidal neurons have been found in this work to be

highly stained with anti-Cb_5R isoform 3 and anti-Cb_5 (Fig. 11). Noteworthy, the soma of these pyramidal neurons was more heavily stained with anti-Cb_5R isoform 3 and anti-Cb_5 than their extensions. Similar to neurogranin staining, the expression level of Cb_5R isoform 3 is also observable in apical dendrites (in the *stratum radiatum*) and seems to be higher than Cb_5 expression, while the basal dendrites (in the *stratum oriens*) appeared scarcely stained with anti-Cb_5R isoform 3 and with anti-Cb_5 (Fig. 11).

AQ2

This specific dendritic and soma expression of Cb_5R isoform 3 and Cb_5 proteins in hippocampus and neocortex brain areas playing a key role in synaptic plasticity suggests a yet unraveled role of these proteins in the modulation of normal activity of these relevant brain areas, particularly prone to neurodegeneration in aging and Alzheimer's disease. This is in good agreement with recent studies, emphasizing the surprising level of precision exhibited by synapses within the neocortex and hippocampus (Higley 2014). Specifically, inhibitory GABAergic system of pyramidal cells plays a key role in the localized regulation of neuronal Ca^{2+} signaling.

Conclusions

The high expression levels of Cb_5R isoform 3 and Cb_5 found in Purkinje cells and in large pyramidal neurons of brain stem motor nuclei, motor areas of the cerebral neocortex and hippocampus, are novel experimental findings reported in this work. Moreover, the high levels of expression of these proteins found in cerebellar granule neurons in vivo are in excellent agreement with the results obtained with in vitro primary cultures of mature cerebellar granule neurons and reported in previous works of our laboratory. Purkinje cells play a major integrative role in cerebellar output response; thus, functional impairment or degeneration of these cells is likely underlying some of the neurological deficits linked with cerebellum dysfunction in recessive congenital methemoglobinemia of type II produced by naturally occurring mutations of the human Cb_5R. As briefly indicated in the introduction, the Cb_5R/Cb_5 system plays a key role in normal lipid metabolism, which is critical to support and maintain the neuronal plasticity associated with a high synaptic activity, and the Cb_5R isoform 3 bound to the plasma membrane catalyzes the NADH-dependent recycling of ascorbate free radical to ascorbate, the major extracellular antioxidant in brain. Thus, Purkinje and cerebellar granule neurons functional activity and ability to

counteract tissular oxidative stress are expected to be largely impaired by Cb_5R mutations leading to loss of function of this protein, thereby being more prone to degeneration.

In addition, we have found that the redox Cb_5R isoform 3/Cb_5 system is highly expressed in several brain stem nuclei that play major neuroanatomical and physiological roles in the control and coordination of the efferent cerebellar pathways. In addition, as this system is also highly expressed in pyramidal neurons of the primary and secondary motor areas of the cerebral cortex and of the hippocampus, these findings bear special relevance for the localization of cerebellar neurons, nuclei and processes more prone to undergo oxidative-induced neuronal death in neurodegenerative insults and diseases whose development is associated with severe motor neurological disorders.

Acknowledgments

AKSA was recipient of a post-doctoral fellowship of the Junta de Extremadura and DMS was recipient of a pre-doctoral fellowship of the Spanish Ministerios de Ciencia e Innovación y Economía y Competitividad. The technical help of Dr. José Antonio Tapia with confocal microscopy images acquisition is gratefully acknowledged. This work has been financed with research project BFU2011-30178 of the Spanish Ministerio de Economía y Competitividad and grants to research groups CCV008/BBB008 and CTS005 of the Plan Regional de I + D+I of the Junta/Gobierno de Extremadura (Spain). These fellowships and grants have been co-financed with the European Fund for Economic and Regional Development (FEDER).

Conflict of interest The authors declare that they have not conflict of interest.

Electronic supplementary material

Below is the link to the electronic supplementary material.

Figure S1. Western blotting of adult rat brain lysates (2.5 μg of protein per lane) **with rabbit anti-Cb_5R isoform 3** (anti-DIA1; Protein Tech Group: 10894-1-AP, dilution 1:100) **and with anti-Cb_5 (**Santa Cruz Biotechnology: sc 33174, dilution 1:100). Details of the experimental protocol are given in the section II.A of Materials and Methods (PPT 151 kb)

Figure S2 (optional, at editor's decision; data also cited in the text as *data not shown*). (I) Control for Figure 1: The primary antibodies were replaced with rabbit IgG and slices were later treated with the secondary antibody used for the immunohistochemistry images (biotinylated goat anti-rabbit IgG). Raw light micrographs images of coronal sections at cerebellar and brain stem level showed lack of significant staining with biotinylated goat anti-rabbit IgG (A-C) when compared with the staining observed after immunohistochemistry with anti-Cb_5R isoform 3 (A-C images shown in the Figure 1) and anti-Cb_5 (D-F images shown in the Figure 1). Scale bars: I-A (1 mm), I-B (200 μm) and I-C (100 μm). Similar images were obtained using the secondary antibody alone. **(II) Control for Figure 3: The primary antibodies were replaced with rabbit IgG and slices were later treated with the secondary antibody used for the immunohistochemistry images (biotinylated goat anti-rabbit IgG).** Raw light micrographs images of coronal sections at cerebellar and brain stem level showed lack of significant staining with biotinylated goat anti-rabbit IgG (A,B) when compared with the staining observed after immunohistochemistry with anti-Cb_5R isoform 3 and anti-Cb_5 (images shown in the Figure 3). Scale bars: II-A (1 mm) and II-B (100 μm). Similar images were obtained using the secondary antibody alone. **(III) Control for Figures 10 and 11**. "Biotinylated goat anti-rabbit IgG" are raw images of controls done with the secondary antibody used for the immunohistochemistry images (biotinylated goat anti-rabbit IgG) alone, and these images showed lack of significant staining with biotinylated goat anti-rabbit IgG when compared with the staining observed after immunohistochemistry with anti-Cb_5R isoform 3 and anti-Cb_5 (images shown in Figures 10 and 11). (**A**) somatomotor areas of cerebral cortex (**Mo**) and hypocampal region (**Hip**) shown with higher magnification in (**B**) and (**C**). Image **B** shows the somatomotor areas of cerebral cortex with higher magnification. Image **C** shows the Ammon´s horn of hypocampal region with higher magnification. Inserted abbreviations in image (**C**): pyramidal layer (p) of Ammon´s horn of hypocampal region (CA1, CA2 and CA3: Pyramidal fields). Scale bars: IIIA (0.75 mm), IIIB (100 μm) and IIIC (100 μm) (PPT 651 kb)

References

Aalfs CM, Salieb-Beugelaar GB, Wanders RJA, Mannens MMAM, Wijburg FA (2000) A case of methemoglobinemia type II due to NADH-cytochrome b_5 reductase deficiency: determination of the molecular basis. Hum Mutat 16:18–22

Borgese N, D'Arrigo A, De Silvestris M, Pietrini G (1993) NADH-cytochrome b_5 reductase and cytochrome b_5 isoforms as models for the study of post-translational targeting to the endoplasmic reticulum. FEBS Lett 325:70–75

Canu N, Calissano P (2003) *In vitro* cultured neurons for molecular studies correlating apoptosis with events related to Alzheimer disease. Cerebellum 2:270–278

Celio MR (1990) Calbindin-D28 k and parvalbumin in the rat nervous system. Neuroscience 35:375–475

Chatenay-Rivauday C, Cakar ZP, Jeno P, Kuzmenko ES, Fiedler K (2004) Caveolae: biochemical analysis. Mol Biol Rep 31:67–84

Contestabile A (2002) Cerebellar granule cells as a model to study mechanisms of neuronal apoptosis or survival in vivo and in vitro. Cerebellum 1:41–55

Crane FL, Sun IL, Crowe RA, Alcain FJ, Low H (1994) Coenzyme Q10, plasma membrane oxidase and growth control. Mol Aspects Med 15(Suppl):s1–11

Dikranian K, Qin YQ, Labruyere J, Nemmers B, Olney JW (2005) Ethanol-induced neuroapoptosis in the developing rodent cerebellum and related brain stem structures. Brain Res Dev Brain Res 155:1–13

Dougherty SE, Reeves JL, Lucas EK, Gamble KL, Lesort M, Cowell RM (2012) Disruption of Purkinje cell function prior to huntingtin accumulation and cell loss in an animal model of Huntington Disease. Exp Neurol 236:171–178

Dusart I, Airaksinen MS, Sotelo C (1997) Purkinje cell survival and axonal regeneration are age dependent: an in vitro study. J Neurosci

17:3710–3726

Elrick MJ, Pacheco CD, Yu T, Dadga N, Shakkottai VG, Ware C, Paulson HL, Lieberman AP (2010) Conditional Niemann-Pick C mice demonstrate cell autonomous Purkinje cell neurodegeneration. Hum Mol Genet 19:837–847

Ewenczyk C, Leroux A, Roubergue A, Laugel V, Afenjar A, Saudubray JM, Beauvais P, Billette de Villemeur T, Vidailhet M, Roze E (2008) Recessive hereditary methaemoglobinaemia, type II: delineation of the clinical spectrum. Brain 131:760–761

Fujita M, Kadota T, Sato T (1996) Developmental profiles of synaptophysin in granule cells of rat cerebellum: an immunohistocytochemical study. J Electron Microsc 45:185–194

Girard M, Larivière R, Parfitt DA, Deane EC, Gaudet R, Nossova N, Blondeau F, Prenosil G, Vermeulen EG, Duchen MR, Richter A, Shoubridge EA, Gehring K, McKinney RA, Brais B, Chapple JP, McPherson PS (2012) Mitochondrial dysfunction and Purkinje cell loss in autosomal recessive spastic ataxia of Charlevoix-Saguenay (ARSACS). Proc Natl Acad Sci USA 109:1661–1666

Harrison FE, May JM (2009) Vitamin C function in the brain: vital role of the ascorbate transporter SVCT2. Free Radic Biol Med 46:719–730

Higley MJ (2014) Localized GABAergic inhibition of dendritic Ca(2+) signalling. Nat Rev Neurosci 15:567–572

Hildebrandt A, Estabrook RW (1971) Evidence for the participation of cytochrome b5 in hepatic microsomal mixed-function oxidation reactions. Arch Biochem Biophys 143:66–79

Hourez R, Servais L, Orduz D, Gall D, Millard I, de Kerchove d'Exaerde A, Cheron G, Orr Orr, Pandolfo M, Schiffmann SF (2011) Aminopyridines correct early dysfunction and delay neurodegeneration in a mouse model of spinocerebellar ataxia type 1. J Neurosci 31:11795–11807

Huang Y, Tai C, Lu Y, Wu TJ, Chen H, Niu D (2012) Recessive congenital methemoglobinemia caused by a rare mechanism: maternal uniparental heterodisomy with segmental isodisomy of a chromosome 22. Blood Cells Mol Dis 49:114–117

Hultquist DE, Passon PG (1971) Catalysis of methaemoglobin reduction by erythrocyte cytochrome b_5 and cytochrome b_5 reductase. Nat New Biol 229:252–254

Janes PW, Ley SC, Magee AI (1999) Aggregation of lipid rafts accompanies signalling via the T cell antigen receptor. J Cell Biol 147:447–461

Jeffcoat R, Brawn PR, Safford R, James AT (1977) Properties of rat liver microsomal stearoyl-coenzyme A desaturase. Biochem J 161:431–437

Kasumu A, Bezprozvanny I (2012) Deranged calcium signaling in purkinje cells and pathogenesis in spinocerebellar ataxia 2 (SCA2) and OTHER ataxias. Cerebellum 11:630–639

Kawata S, Trzaskos JM, Gaylor JL (1985) Microsomal enzymes of cholesterol biosynthesis from lanosterol. Purification and characterization of delta 7-sterol 5-desaturase of rat liver microsomes. J Biol Chem 260:6609–6617

Lagoa R, López-Sánchez C, Samhan-Arias AK, Gañán CM, García-Martínez V, Gutierrez-Merino C (2009) Kaempferol protects against rat striatal degeneration induced by 3-nitropropionic acid. J Neurochem 111:473–487

Leroux A, Junien C, Kaplan J, Bambenger J (1975) Generalised deficiency of cytochrome b_5 reductase in congenital methaemoglobinaemia with mental retardation. Nature 258:619–620

López-Sánchez C, Martín-Romero FJ, Sun F, Luis L, Samhan-Arias AK, García-Martínez V, Gutierrez-Merino C (2007) Blood micromolar concentrations of kaempferol afford protection against ischemia/reperfusion-induced damage in rat brain. Brain Res 1182:123–

Marques-da-Silva D, Gutierrez-Merino C (2012) L-type voltage-operated calcium channels, N-methyl-D-aspartate receptors and neuronal nitric oxide synthase form a calcium/redox nano-transducer within lipid rafts. Biochem Biophys Res Commun 420:257–262

Marques-da-Silva D, Gutierrez-Merino C (2014) Caveolin-rich lipid rafts of the plasma membrane of mature cerebellar granule neurons are microcompartments for calcium/reactive oxygen and nitrogen species cross-talk signaling. Cell Calcium 56:108–123

Marques-da-Silva D, Samhan-Arias AK, Tiago T, Gutierrez-Merino C (2010) L-type calcium channels and cytochrome b_5 reductase are components of protein complexes tightly associated with lipid rafts microdomains of the neuronal plasma membrane. J Proteomics 73:1502–1510

Martin-Romero FJ, Garcia-Martin E, Gutierrez-Merino C (2002) Inhibition of oxidative stress produced by plasma membrane NADH oxidase delays low-potassium-induced apoptosis of cerebellar granule cells. J Neurochem 82:705–715

May JM (1999) Is ascorbic acid an antioxidant for the plasma membrane? FASEB J 13:995–1006

Nakamura A, Uchihara T (2004) Dual enhancement of triple immunofluorescence using two antibodies from the same species. J Neurosci Methods 135:67–70

ÓCallagan JP (1988) Neurotypic and gliotypic proteins and biochemical markers of neurotoxicity. Neurotoxicol Teratol 10:445–452

ÓConnell KMM, Martens JR, Tamkun MM (2004) Localization of ion channels to lipid raft domains within the cardiovascular system. Trends Cardiovasc Med 14:37–42

Paine MG, Che G, Li M, Neumar RW (2012) Cerebellar Purkinje cell neurodegeneration after cardiac arrest: effect of therapeutic hypothermia.

Resuscitation 83:1511–1516

Percy MJ, Lappin TR (2008) Recessive congenital methaemoglobinaemia: cytochrome b5 reductase deficiency. Br J Haematol 141:298–308

Pilati N, Barker M, Panteleimonitis S, Donga R, Hamann M (2008) A rapid method combining Golgi and Nissl staining to study neuronal morphology and cytoarchitecture. J Histochem Cytochem 56:539–550

Represa A, Deloulme JC, Sensenbrenner M, Ben-Ari Y, Baudier J (1990) Neurogranin: immunocytochemical localization of a brain-specific protein kinase C substrate. J Neurosci 10:3782–3792

Rioux V, Pédrono F, Legrand P (2011) Regulation of mammalian desaturases by myristic acid: n-terminal myristoylation and other modulations. Biochim Biophys Acta 1811:1–8

Roda E, Coccini T, Acerbi D, Castoldi A, Bernocchi G, Manzo L (2008) Cerebellum cholinergic muscarinic receptor (subtype-2 and -3) and cytoarchitecture after developmental exposure to methylmercury: an immunohistochemical study in rat. J Chem Neuroanat 35:285–294

Saab AS, Neumeyer A, Jahn HM, Cupido A, Šimek AA, Boele HJ, Scheller A, Le Meur K, Götz M, Monyer H, Sprengel R, Rubio ME, Deitmer JW, De Zeeuw CI, Kirchhoff F (2012) Bergmann glial AMPA receptors are required for fine motor coordination. Science 337:749–753

Samhan-Arias AK, Gutierrez-Merino C (2014a) Purified NADH-cytochrome b_5 reductase is a novel superoxide anion source inhibited by apocynin: sensitivity to nitric oxide and peroxynitrite. Free Radic Biol Med 73:174–189

Samhan-Arias AK, Gutierrez-Merino C (2014) Cytochrome b_5 as a pleiotropic metabolic modulator in mammalian cells. In: Rurik Thom (ed) Cytochromes *b* and *c*: Biochemical properties, biological functions and electrochemical analysis, Chapter 2, Nova Science Publishers, Hauppauge, pp. 39–80

Samhan-Arias AK, Martin-Romero FJ, Gutierrez-Merino C (2004)

Kaempferol blocks oxidative stress in cerebellar granule cells and reveals a key role for reactive oxygen species production at the plasma membrane in the commitment to apoptosis. Free Radical Biol Med 37:48–61

Samhan-Arias AK, Duarte RO, Martín-Romero FJ, Moura JJ, Gutierrez-Merino C (2008) Reduction of ascorbate free radical by the plasma membrane of synaptic terminals from rat brain. Arch Biochem Biophys 469:243–254

Samhan-Arias AK, Garcia-Bereguiain MA, Martin-Romero FJ, Gutierrez-Merino C (2009) Clustering of plasma membrane-bound cytochrome b5 reductase within 'lipid raft' microdomains of the neuronal plasma membrane. Mol Cell Neurosci 40:14–26

Samhan-Arias AK, Marques-da-Silva D, Yanamala N, Gutierrez-Merino C (2012) Stimulation and clustering of cytochrome b_5 reductase in caveolin-rich lipid microdomains is an early event in oxidative stress-mediated apoptosis of cerebellar granule neurons. J Proteomics 75:2934–2949

Sasaki S, Yoshimura K, Naito K (2004) The neural control of orienting: role of multiple-branching reticulospinal neurons. Prog Brain Res 143:383–389

Schenkman JB, Jansson I (2003) The many roles of cytochrome b_5. Pharmacol Ther 97:139–152

Stephenson DT, Kushner PD (1988) An atlas of a rare neuronal surface antigen in the rat central nervous system. J Neurosci 8:3035–3056

Storbeck KH, Swart AC, Lombard N, Adriaanse CV, Swart P (2012) Cytochrome b_5 forms homomeric complexes in living cells. J Steroid Biochem Mol Biol 132:311–321

Taft JR, Vertes RP, Perry GW (2005) Distribution of GFAP+ astrocytes in adult and neonatal rat brain. Int J Neurosci 115:1333–1343

Toelle SP, Boltshauser E, Mossner E et al (2004) Severe neurological impairment in hereditary methaemoglobinaemia type 2. Eur J Pediatr

163:207–209

Valencia A, Moran J (2001) Role of oxidative stress in the apoptotic cell death of cultured cerebellar granule neurons. J Neurosci Res 64:284–297

Vieira LM, Kaplan JC, Kahn A, Leroux A (1995) Four new mutations in the NADH-cytochrome b5 reductase gene from patients with recessive congenital methemoglobinemia type II. Blood 85:2254–2262

Villalba JM, Navarro F, Gómez-Díaz C, Arroyo A, Bello RI, Navas P (1997) Role of cytochrome b_5 reductase on the antioxidant function of coenzyme Q in the plasma membrane. Mol Aspects Med 18(Suppl):S7–S13

Wang F, Xu Q, Wang W, Takano T, Nedergaard M (2012) Bergmann glia modulate cerebellar Purkinje cell bistability via Ca^{2+}-dependent K^+ uptake. Proc Natl Acad Sci USA 109:7911–7916